Polymer Diffusion in PBMA Latex Films Using a Polymerizable Benzophenone Derivative as an Energy Transfer Acceptor

Xiaodong Ye,[†,‡] J. P. S. Farinha,[§] Jung Kwon Oh,[‡] Mitchell A. Winnik,*,[‡] and Chi Wu[†,⊥]

The Opening Laboratory for Bond-Selective Chemistry, Department of Chemical Physics, University of Science and Technology of China, Hefei, Anhui 230026, China, Department of Chemistry, University of Toronto, 80 Saint George Street, Toronto, Ontario, Canada M5S 3H6, Centro de Química-Física Molecular, Instituto Superior Tecnico, 1049-001 Lisboa, Portugal, and Department of Chemistry, The Chinese University of Hong Kong, Shatin, N.T., Hong Kong

ABSTRACT: Fluorescence resonance energy transfer (FRET) measurements were used to monitor polymer diffusion in poly(butyl methacrylate) latex films with a polymer molar mass of $M_w \approx 125\,000$ ($M_w/M_n = 2.5$). These experiments employed the nonfluorescent acceptor chromophore NBen, which allowed faster data acquisition at lower acceptor dye concentration (0.3, 0.5 mol %) than previous experiments with anthracene (1 mol %) as the acceptor. The data were analyzed in two distinct ways. Our traditional simplified approach involved calculating f_m values for the quantum efficiencies of FRET (Φ_{ET}). Apparent diffusion coefficients D_{app} were calculated by making rather severe assumptions about f_m. In addition, we carried out mathematical simulations of diffusion which satisfied Fick's laws in a spherical geometry. The concentration profiles of donor and acceptor were introduced into equations that describe the rate for of energy transfer, and donor decay profiles were simulated $I_D^s(t)$. By comparing simulated and experimental decay profiles as a function of sample annealing time, optimum values of the mean diffusion coefficient $\langle D \rangle$ were obtained. A comparison of the two different methods of data analysis indicates that D_{app} values are larger than $\langle D \rangle$ values by a factor of 2−4 but track the "true" diffusion coefficients rather well. From the temperature dependence of the diffusion coefficients, we found effective activation energies for diffusion of $E_a = 33.5 \pm 2.5$ kcal/mol from D_{app} and 38 ± 5 kcal/mol from $\langle D \rangle$. These values are very similar to the value of $E_a = 39$ kcal/mol from D_{app} obtained in earlier experiments in which anthracene served as the acceptor chromophore.

Introduction

For more than a decade, we have employed fluorescence resonance energy transfer (FRET) experiments to study polymer diffusion in latex films. Most of the systems examined involved linear poly(butyl methacrylate) (PBMA) and its copolymers, where we have investigated temperature effects,[1] molecular weight effects,[2] surfactant effects,[3] moisture effects,[4] and the influence of other factors such as plasticizers,[5,6] polar groups at the latex surface.[7] In these systems, we normally used phenanthrene (Phe) as donor dye and anthracene (An) as the acceptor dye. These dyes were incorporated into the latex particles via dye comonomers with methacrylates or vinyl substituents.

In most of these experiments, we used 9-phenanthrylmethyl methacrylate (PheMMA) (**1**) as the dye comonomer in the synthesis of donor-labeled PBMA latex particles. This dye works very well for emulsion copolymerization of both methacrylate and acrylate monomers. In contrast, the synthesis of acceptor-labeled latex particles was not as straightforward. For reasons that are not completely understood, the anthracene (An) derivatives often inhibit the polymerization. In the past we have been able to overcome this problem by the proper choice of An derivatives. For methacrylates such as butyl methacrylate or methyl methacrylate, we have

used **2** successfully. For acrylates such as butyl acrylate, it was necessary to use An derivatives such as **3**, in which a methyl group or alkyl group blocks the 10-position of the anthracene.
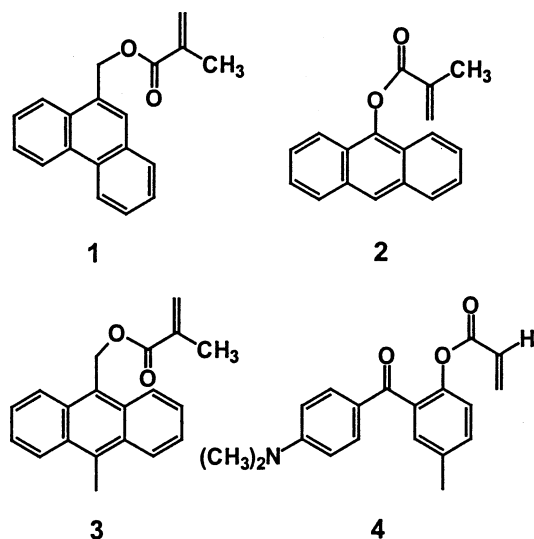
Recently, we began a project that required labeled latex consisting of a 4/1 (w/w) vinyl acetate−butyl acrylate (VAc−BA) copolymer. There were some problems in the synthesis of labeled latex particles. For example, in the synthesis of donor-labeled latex particles, the methacrylate **1** led to incomplete monomer conversion. This problem was relatively easily overcome by using the corresponding acrylate derivative. With

---

* To whom correspondence should be addressed. E-mail: mwinnik@chem.utoronto.ca.
† University of Science and Technology of China.
‡ University of Toronto.
§ Instituto Superior Tecnico.
⊥ The Chinese University of Hong Kong.

this dye, monomer conversion reached more than 95% and useful donor-labeled particles were obtained. We were unable, however, to obtain useful anthracene-labeled particles. All anthracene derivatives we examined inhibited or suppressed monomer polymerization. To proceed with these studies, we undertook a search for new dyes that could act as energy-transfer acceptors from Phe and at the same time would not inhibit VAc−BA copolymerization. The most successful candidates were 4-(dimethylamino)benzophenone (NBen) derivatives such as **4**.[8] This dye has a number of interesting advantages over An derivatives as an acceptor for energy transfer experiments with Phe as the donor chromophore. First, it copolymerizes effectively with a broader range of monomers. Second, it appears to have a slightly larger characteristic energy transfer distance (Förster radius R_0) for Phe as the donor;[1] thus FRET experiments can be carried out with smaller levels of polymer labeling. Finally, **4** is nonfluorescent. As a consequence, one can monitor Phe emission over its entire emission spectrum without concern for competing emission from the acceptor dye.

We have begun to explore the utility of the Phe/NBen donor−acceptor pair for a variety of different experiments involving latex films. To put these experiments on a firmer footing, we have chosen to go back to latex films consisting of linear poly(butyl methacrylate) (PBMA). Since we have obtained deeper knowledge about polymer diffusion in PBMA latex films than in any other latex system, these studies can serve as a test platform for assessing the Phe/NBen chromophore pair for FRET studies of polymer diffusion in latex films.

In this paper, Förster critical radii (R_0) between Phe and NBen are calculated by fitting the Phe fluorescence intensity decay profile to the Förster model. We obtained $R_0 = 2.67$ nm when the acceptors were free and $R_0 = 2.37$ nm when both the acceptors and the donors were attached to the polymer. We describe experiments in which we incorporated (9-phenanthyl)methyl methacrylate (PheMMA) and 4′-dimethylamino-2-acryloxy-5-methylbenzephenone (NBen) into a PBMA latex and study polymer diffusion at four different temperatures. We also examine the influence of acceptor concentration on these experiments.

We analyze our data by two methods. First, we evaluate polymer diffusion in the latex films from the evolution of the energy transfer quantum efficiency. We approximate the fractional mass that has diffused across the particle boundary by the normalized energy transfer quantum efficiency. This approach gives us the mean apparent diffusion coefficient D_{app}. We next consider a more fundamental model that describes the shape of the donor fluorescence decay profile, accounting for the density profile of the diffusing polymer and the detailed mechanism of energy transfer from the donor to the acceptor dyes. We fit our experimental donor fluorescence decays with curves simulated by this model. From the polymer segment density profile thus obtained, we determine average diffusion coefficients $\langle D \rangle$ for the polymer as a function of annealing time. Experiments carried out at 56. 74, 90, and 107 °C, were analyzed in terms of D_{app} to give an apparent activation energy $E_a = 33.5 \pm 2.5$ kcal/mol. When the experiments at the three lowermost temperatures were analyzed by the detailed model, we obtained an activation energy of 38 ± 5 kcal/mol.

Table 1. Recipes for the Synthesis of Dye-Labeled PBMA Latex Particles

	first stage[a]	second stage (NBen, 0.3 or 0.5 mol %)	second stage (Phe, 1 mol %)
seeds		14 mL	14 mL
H_2O	2280 g	100 g	100 g
KPS	1.67 g	0.070 g	0.070 g
SDS	26.96 g	0.698 g	0.698 g
$NaHCO_3$	1.17 g	0.401 g	0.401 g
BMA	55.67 g	25.00 g	25.00 g
EGDMA	58.33 g		
NBen (**4**)[b]		0.163 or 0.273 g	
PheMMA			0.486 g
$C_{12}SH$		0.10 mL or 0.090 mL[c]	0.10 mL
diameter	21 nm	120 or 130 nm	120 nm

[a] This seed latex was used for all emulsion polymerization reactions reported here. [b] 0.3 or 0.5 mol % based on total monomer. [c] For NBen(0.5%)-PBMA latex.

Experimental Section

Materials. All reagents were purchased from Aldrich unless otherwise specified. Butyl methacrylate (BMA) and ethylene glycol dimethacrylate (EGDMA) were distilled under vacuum prior to use. Potassium persulfate (KPS), sodium bicarbonate ($NaHCO_3$), dodecyl mercaptan ($C_{12}SH$), sodium dodecyl sulfate (SDS), and dichloromethane were used as received. (9-Phenanthyl)methyl methacrylate (PheMMA) was purchased from Toronto Research Chemicals Inc. and the synthesis and characterization of the monomer 4′-dimethylamino-2-acryloxy-5-methylbenzephenone (NBen) are described elsewhere.[8] Distilled water was further purified through a Millipore Milli-Q system. Particle size and size distributions were measured by dynamic light scattering by a Brookhaven BI-90 particle sizer. Gel permeation chromatography (GPC) was performed on a Waters liquid chromatograph equipped with a Waters 480 tunable UV−vis absorbance detector and a Waters R410 differential refractive detector. The molecular weight was calibrated with poly(methyl methacrylate) standards (Polymer Laboratories Ltd.).

Latex Preparation. All latex dispersions were prepared by seeded semicontinuous emulsion polymerization. Typical recipes are given in Table 1. Cross-linked unlabeled latex seed particles were prepared from a 4/3 molar ratio of BMA and EGDMA by batch emulsion polymerization at 80 °C.[9] The polymerization was carried out under nitrogen in a 3.0-L, three-necked glass reactor fitted with a condenser and a mechanical stirrer. The monomers, surfactant, and $NaHCO_3$ were mixed with water. The mixture, while being stirred mechanically, was degassed by nitrogen bubbling for at least 30 min and then heated to 80 °C. Then the initiator KPS solution was rapidly added. Stirring was continued for another 2−3 h under nitrogen; the dispersion of seed particles ($d = 21$ nm, 5 wt % solids content) was obtained. The same seeds were used for the preparation of all the latex particles, and the seed particles represent 3 wt % of the final latex.

A specific example is provided for the preparation of latex NBen(0.3%)-PBMA. In this notation, (0.3%) refers to the mole percent of dye in the latex polymer. In the second-stage polymerization, an aliquot (14 mL) of the seed dispersion was introduced into a 250-mL three-neck flask equipped with a condenser and a mechanical stirrer. The dispersion was purged with N_2 for 30 min and then heated to 80 °C under N_2. KPS solution was fed quickly into the reactor. Then a preemulsion containing BMA, dye monomer, dodecyl mercaptan, SDS, and water was introduced into the reactor at a constant feed rate (10 mL/h) over 4−5 h. After the addition was complete, the reaction mixture was stirred and heated for another 2 h. This reaction produced a dispersion with 19 wt % solids content with a particle diameter of 130 nm.

Film Formation. Latex films were prepared from dispersion mixtures of 1:1 weight ratio of Phe- and NBen-labeled particles. The dispersions were first cleaned by treating them with a prepurified[10] ion-exchange resin (AG-501-X8 mixed-bed-resin, Bio-Rad) to remove the ionic surfactant and other ionic

Table 2. Bulk Acceptor Concentration [Q] of Samples Used To Determine the Förster Radius R_0

sample[a]	[Q], mM	sample[b]	[Q], mM
NBen1	5.22	NBen7	4.43
NBen2	7.90	NBen8	7.56
NBen3	9.84	NBen9	9.17
NBen4	12.63	NBen10	10.71
NBen5	16.43	NBen11	17.89
NBen6	18.17		

[a] The monomer **4** is the acceptor. [b] The acceptor NBen is attached to the PBMA polymer in these films.

species before film formation. A few drops of a latex dispersion (containing 1:1 ratio of mixed Phe- and NBen-labeled particle, 6 wt % solids) were spread on a small quartz plate. The film was allowed to dry at room temperature in the open air for one night before annealing. Films were dry and transparent. For the films that were used to measure the Förster radius R_0 for energy transfer between Phe and NBen, a series of solutions were prepared by adding different amounts of NBen (**4**) in dichloromethane to solutions of Phe-labeled PBMA in dichloromethane. A few drops of each of these solutions were spread on six small quartz plates and allowed to dry. The bulk concentrations of **4** in these films are listed in Table 2. For experiments to determine the R_0 value where both donors and acceptors were attached to the PBMA polymer, different weight ratios of freeze-dried powder of PBMA labeled with donor or acceptor were dissolved in THF, then a few drops of each of these solution were spread on quartz plates.

Fluorescence Measurements. All fluorescence decay profiles were measured by the time-correlated single photon counting technique.[11] The measurements were conducted at room temperature. The donor phenanthrene was excited at 300 nm, and its emission was recorded over the range 350–400 nm. A band-pass filter (310–400 nm) and a cutoff filter (335 nm) were mounted in the front of the photomultiplier tube detector to minimize the interference due to scattered light. For fluorescence decay measurements, each sample was placed in a small quartz tube and degassed with flowing N_2 for 5 min before each measurement. Control experiments showed a slightly smaller integrated area under the donor decay profile for films exposed to air, equivalent to an apparent increase of 0.03 in "energy transfer efficiency" between the film before degassing and the same film after flushing with nitrogen gas. In the absence of NBen as an energy transfer acceptor, Phe decay profiles were exponential, with $\tau_D = 46.1$ ns for the Phe(1%)–PBMA latex film.

Data and Data Analysis

For a dipole–dipole coupling mechanism, the rate of energy transfer $w(r)$ between a donor and an acceptor molecule depends on the inverse sixth power of their separation distance r,[12]

$$w(r) = \frac{\alpha}{r^6} \tag{1a}$$

$$\alpha = \frac{3R_0^6\kappa^2}{2\tau_D} \tag{1b}$$

Here, τ_D is the unquenched donor lifetime and R_0 is the characteristic (Förster) energy transfer distance defined as[13]

$$R_0^6 = \frac{9000(\ln10)\kappa^2 Q_D}{128\pi^5 N_A n^4} \int_0^\infty F_D(\lambda)\epsilon_A(\lambda)\lambda^4\,d\lambda \tag{2}$$

where κ^2 is a dimensionless parameter related to the relative orientation of the donor and acceptor transition dipole moments,[14] Q_D is the quantum yield of the donor

in the absence of acceptor, N_A is Avogadro's number, n is the refractive index of the medium, $F_D(\lambda)$ is fluorescence intensity of the donor at wavelength λ (with the total intensity normalized to unity), and $\epsilon_a(\lambda)$ is the extinction coefficient of the acceptor at λ.

If the donors and acceptors are homogeneously distributed in a three-dimensional Euclidean space, the donor decay function will have the stretched exponential form derived by Förster.[12,13]

$$I_D(t) = I_D(0)\exp\left(-\frac{t}{\tau_D}\right)\exp\left[-P\left(\frac{t}{\tau_D}\right)^{1/2}\right] \tag{3}$$

where t is the fluorescence decay time, and the parameter P depends on the concentration of acceptors [A] and on the averaged relative orientation $\langle\kappa^2\rangle$ of the donor and acceptor transition moments.

$$P = \frac{4}{3}\pi^{3/2}N_A\left(\frac{3}{2}\langle\kappa^2\rangle\right)^{1/2}R_0^3[A] \tag{4}$$

In writing eqs 1 and 4, we take account of the common practice of defining R_0 in terms of an experiment with rapidly rotating dipoles in which $\langle\kappa^2\rangle = 2/3$. The experiments described here involve a random distribution of dipoles that are immobile on the time scale of the donor lifetime. For this case, $\langle\kappa^2\rangle = 0.476$.[14]

Under some circumstances (e.g., from simulations), one has independent knowledge of the donor and acceptor concentration profiles in a system. These concentration profiles can be related to the donor survival probability through the theory of energy transfer in restricted geometry.[15,16] For diffusion across an interface, the spatial distribution of donors and acceptors is nonhomogeneous, and therefore the donor fluorescence decay rate depends on both the distribution of acceptors around each donor and the distribution of donors itself. For a delta-pulse excitation the probability $\check{I}_D(t)$ is described by[16]

$$\check{I}_D(t) = \exp\left(-\frac{t}{\tau_D}\right)\int_{V_s}C_D(r_D)\varphi(t,r_D)r_D^2\,dr_D \tag{5a}$$

$$\varphi(t,r_D) =$$
$$\exp\left(-\frac{2\pi}{r_D}\int_{R_e}^\infty\{1-\exp[-w(r)t]\}[\int_{|r_D-r|}^{r_D+r}C_A(r_A)r_A\,dr_A]r\,dr\right) \tag{5b}$$

where V_s is the volume containing the donors initially confined to a donor labeled particle. φ (t, r_D) is the probability of energy transfer of a donor located at r_D. The encounter radius, R_e, is the minimum distance between donor and acceptor at which the effect of dipolar energy transfer can still be observed in the donor fluorescence. It is usually set equal to the sum of the donor and acceptor van der Waals radii.[17]

To analyze experimental data through simulations, one convolutes the trial decay function $\check{I}_D(t)$ with the experimental lamp function and compares the resulting simulated fluorescence decay curve with the measured curve. We modify the input parameters to the simulation to obtain the best fit as determined by minimization of χ^2. Good fits are characterized by a random distribution of both the weighted residuals and the autocorrelation of weighted residuals.

The quantum efficiency of energy transfer $\Phi_{ET}(t)$ can be evaluated from the donor fluorescence decay profiles

$I_D(t)$ for films in the presence and absence of acceptors.

$$\Phi_{ET} = 1 - \frac{\int_0^\infty I_D(t)\, dt}{\int_0^\infty I_D^0(t)\, dt} = 1 - \frac{\text{Area}(t_{dif})}{\text{Area(D)}} \quad (6)$$

The middle term represents the definition of the energy transfer efficiency in terms of the integrated intensity decay profiles, where $I_D^0(t)$ is the donor decay profile in the absence of acceptor. For latex films containing phenanthrene as the donor, $I_D^0(t)$ is always exponential. Area(t_{dif}) represents the integrated area under the fluorescence decay profile of a latex film sample annealed for a time t_{dif}, and Area(D) refers to the area under the decay profile of a film containing only donor. Polymer diffusion leads to complex profiles of D and A groups, for which eq 3 would not be expected to apply. To obtain an accurate area for each decay profile, we fit each decay curve to the expression

$$I_D(t) = A_1 \exp[-t/\tau_0 - p(t/\tau_0)^{1/2}] + A_2 \exp(-t/\tau_0) \quad (7)$$

In eq 7, unlike eq 3, the fitting parameters do not have an intrinsic scientific meaning. We use these fitting parameters only to evaluate the magnitude of the integral in the numerator of eq 6. All fits in this article have goodness-of-fit χ^2 values less than 1.3.

We define the extent of mixing f_m that occurs upon annealing a sample for a time t_{dif} in terms of the fractional evolution of the quantum efficiency of energy transfer

$$f_m = \frac{\Phi_{ET}(t_{dif}) - \Phi_{ET}(t_0)}{\Phi_{ET}(t_\infty) - \Phi_{ET}(t_0)} = \frac{\text{Area}(t_0) - \text{Area}(t_{dif})}{\text{Area}(t_0) - \text{Area}(t_\infty)} \quad (8)$$

In eq 8, $[\Phi_{ET}(t_{dif}) - \Phi_{ET}(t_0)]$ represents the change in energy transfer efficiency between the freshly prepared film and that annealed for time t_{dif} and $[\Phi_{ET}(t_\infty) - \Phi_{ET}(t_0)]$ is the difference in energy transfer efficiency between the fully mixed film and the newly formed film. To obtain values of $\Phi_{ET}(t_\infty)$, representing full mixing, we took a latex film sample, dissolved it in THF, and then recast a film onto a quartz plate. $\Phi_{ET}(t_\infty)$ was 0.37 for films prepared with NBen(0.3%)-PBMA, and 0.52 for films prepared with NBen(0.5%)-PBMA.

Results and Discussion

Preparation and Characterization of the Latex Samples. In our approach to the study of polymer diffusion in latex films by FRET experiments, we prepare films from a blend of donor- and acceptor-labeled latex particles. The data analysis is based on the assumption that the donor and acceptor dyes serve only as traces for the location of the polymer. Thus it is important that the two types of latex particles be very similar in particle size and in the molecular weight and molecular weight distribution of their constituent polymers. This result is most easily achieved if both types of particles are synthesized from a common unlabeled seed latex. The characteristics of the samples we prepared are listed in Table 3. Because the three labeled latex dispersion were prepared with nearly identical recipes and under essentially identical conditions, we obtained particles of similar size. The molecular weights and molecular weight distribution of the three types of particles were also very similar. Figure 1 shows a GPC

Table 3. Latex Particle Characteristics

|	Phe(1%)-PBMA	NBen(0.3%)-PBMA	NBen(0.5%)-PBMA
M_w	122 000	120 000	129 000
M_w/M_n	2.5	2.6	2.4
D, nm	130	120	130
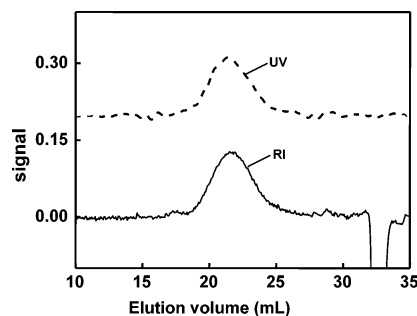
Figure 1. GPC curves for NBen(0.3%)-PBMA sample: RI signal and UV signal.

trace for the NBen(0.3%)-PBMA sample. The continuous line represents the RI signal, which indicates the elution of the polymer. The UV signal, shown as a dashed line, indicates the elution of the NBen chromophore. Both signals exhibit a peak at 19−26 min with a similar shape, indicating random dye distribution in the polymer. In the low molar mass region, there is no signal in the UV trace. Thus, there is no low molar mass NBen species in the sample. We conclude from this result that all the dye comonomer was incorporated into the polymer.

Determination of R_0. One of the advantages of NBen over An as an acceptor of FRET from Phe is that it has a higher extinction coefficient in the region of the phenanthrene fluorescence. The monomer **4** has an extinction coefficient of 24 500 L mol^{-1} cm^{-1} at 350 nm (l_{max}, CHCl$_3$), whereas that of the An-methacrylate derivative **2** is closer to 8000 L mol^{-1} cm^{-1} at l_{max} = 359 nm. This difference translates into a larger overlap integral when we use NBen as the acceptor. One of the disadvantages of NBen as an acceptor chromophore is that the excitation at 349 nm is due to a charge-transfer transition. While we do not observe large shifts in the position of this maximum as a function of the polarity of the medium, small shifts in λ_{max} and possible changes in the molar extinction coefficient make it difficult at present to obtain a unique value for R_0 for FRET from Phe as the donor.

R_0 values for polymer-bound chromophores are normally determined by reference to model compounds. In the traditional approach, one examines solutions of the dyes in an organic solvent. One measures the unquenched fluorescence quantum yield of the donor and carries out careful measurements of the absorption spectrum of the acceptor and the emission spectrum of the donor. From the quantum yield and the overlap integral, one calculates the R_0 value for the donor−acceptor pair in solution (eq 2). While this approach has merit, it does not describe the donor−acceptor pair in the polymer matrix, where spectral shifts and a difference in index of refraction can lead to a change in the magnitude of R_0.

An alternative approach involves the use model compounds that, through solvent casting, are dissolved directly in the polymer of interest. One prepares a series of solutions and monitors the donor decay profile as a function of the bulk concentration of the acceptor dye.
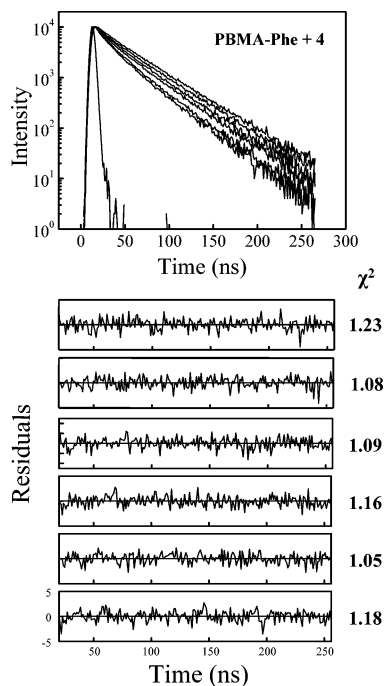
Figure 2. Fluorescence decay profiles for PBMA-Phe samples with different amounts of free acceptor **4** and the corresponding weighted residuals and χ^2 (From top to bottom samples NBen1 to NBen5, Table 2). The *y*-axis scale is the same for each of the weighted residual plots.

Individual donor decays are fitted to eq 3, and one tests the validity of the results by plotting the fitting parameter *P* against the acceptor concentration [A]. From the slope of this line, one calculates a value for R_0 with eq 4. There are three ways that one could carry out this experiment. First, one could prepare films of an unlabeled polymer containing a model donor dye and various concentrations of a model acceptor dye. Second, one could prepare films in which the donor dye is covalently bound to the polymer and the films contain a range of model acceptor dye concentrations. Both examples should lead to films in which there is a random distribution of acceptor dyes in the matrix, satisfying the assumptions necessary for the proper application of eqs 3 and 4. Third, one could prepare films with various mixtures of donor-labeled polymer and acceptor-labeled polymer. This third approach has the advantage that it represents exactly the FRET experiment used to monitor polymer diffusion. It has the disadvantage that, for high molecular weight polymer, correlation effects (the "correlation hole") will lower the probability of finding an acceptor dye on one polymer in the vicinity of an excited donor dye on another polymer molecule.[18]

We have carried out two such experiments. For the case of donor-labeled polymer + model compound, we prepared six films using the Phe-labeled polymer as the matrix containing different concentrations of the NBen monomer **4** as the model compound. Fluorescence decay curves measured for the films prepared in this way are shown in Figure 2. The decays fit well to eq 3, as shown by the plots of the weighted residuals beneath the decay curves. In a second set of experiments, we prepared films by solution casting various mixtures of the Phe- and NBen-labeled PBMA polymers. The fluorescence decay profiles from these films with different concentrations of the NBen-chromophore are presented in Figure 3, along with plots of the weighted residuals. Here, as well, all of the traces give excellent fits to eq 2.
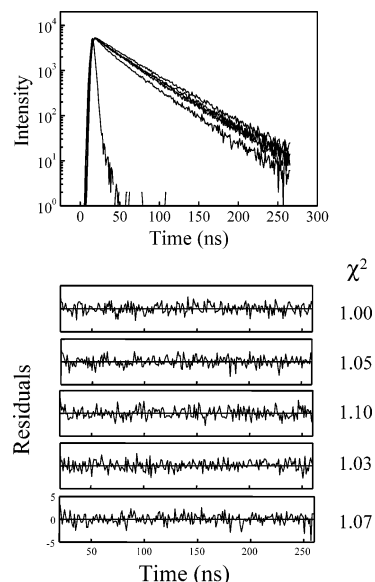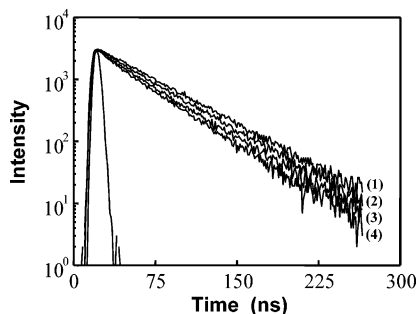

Figure 3. Fluorescence decay profiles and the corresponding weighted residuals for PBMA-Phe PBMA-NBen mixtures. (From top to bottom samples NBen7 to NBen11, Table 2.) The *y*-axis scale is the same for each of the weighted residual plots.
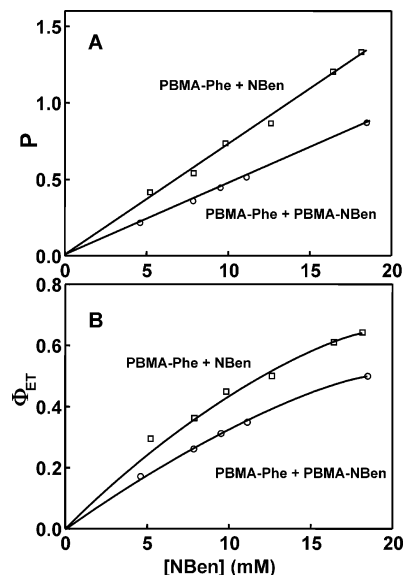

Figure 4. (A) Plots of *P* versus the bulk acceptor concentration [NBen]. Upper line: Phe-PBMA + various concentrations of the NBen monomer **4**. Lower line: Various mixtures of Phe-PBMA + NBen(0.3)-PBMA. (B) The corresponding energy transfer efficiency values for the films in A.

For both sets of experiments, the plots of *P* versus [NBen] are linear and pass through the origin. Figure 4a also shows that *P* values are higher from the films with the free NBen monomer as the model compound than from the films in which both dyes are covalently attached to different polymers. We emphasize this point by calculating the corresponding energy transfer quantum efficiencies Φ_{ET} in Figure 4b. Values of Φ_{ET} are larger at comparable bulk NBen concentration for the films with free monomer as the model compound.

To calculate R_0 from the slopes in Figure 4a, we set $\langle \kappa^2 \rangle = 0.476$ in eq 4. For the films with the free NBen monomer **4**, we obtain $R_0 = 2.67$ nm. For the films in which NBen is covalently linked to PBMA, we obtain $R_0 = 2.37$ nm. Whether this decrease in R_0 is due to small changes in the spectroscopic properties of the

Figure 5. Donor fluorescence decay profiles of PBMA latex films. Curve 1: film of Phe-PBMA. Curves 2−4: films prepared from a 1:1 ratio of Phe-PBMA and NBen(0.3)-PBMA latex particles. Curve 2, a nascent film formed at room temperature; curve 3, a film annealed for 61 min at 90 °C; curve 4, a solvent-cast film.
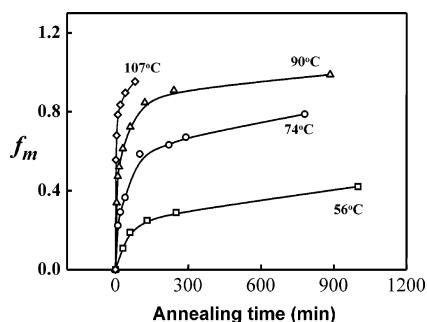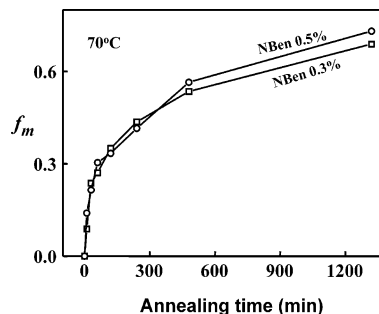

Figure 6. Plots of f_m vs annealing time at different temperatures (56, 74, 90, 107 °C) for latex films consisting of 1:1 ratio of Phe-PBMA and NBen(0.3)-PBMA latex particles.

NBen chromophore or whether it reflects a correlation-hole effect is a matter to be sorted out in future work. We note that the value of 2.67 is larger than the value of 2.3 nm, determined through examination of model compounds, for the Phe/An pair used in our previous experiments.[1]

FRET Experiments on Films with NBen(0.3)-PBMA and NBen(0.5%)-PBMA. In previous experiments with An as the acceptor, we used acceptor-labeled latex containing 0.8−1.0 mol % An groups. In the first set of experiments that we report here, we used acceptor-labeled latex containing 0.3 mol % NBen groups. In Figure 5 we present examples of fluorescence decay curves describing Phe fluorescence decay in the system Phe(1%)-PBMA + NBen(0.3%)-PBMA. The top curve is the exponential decay from a film prepared from the Phe-PBMA latex itself. Curve 2 shows the small degree of curvature associated with a freshly prepared film obtained from a 1:1 mixture of the donor-and acceptor-labeled latex. Curve 3 is that of a film annealed for 61 min at 90 °C, and curve 4 was obtained for a solvent-cast film. It represents full mixing of the donor- and acceptor-labeled polymer.

From the decay curves in Figure 5, we calculate FRET quantum efficiencies of 0.07 for the newly formed film and 0.37 for the solvent-cast film. This range of Φ_{ET} values is sufficient to obtain valid quantitative data from the experiments. Values of f_m calculated from eq 8 are presented in Figure 6 for PBMA film sample annealed at four different temperatures. One can see that the annealing temperature has a large effect on the rate of polymer diffusion, with f_m increasing to 1 in only a few minutes at 107 °C. The growth in f_m becomes substantially slower at lower temperatures.

Figure 7. Plots of f_m vs annealing time at 70 °C for two sets of PBMA latex films with different acceptor concentrations: Phe-PBMA + NBen(0.3%)-PBMA and Phe-PBMA + NBen-(0.5%)-PBMA.

To test the sensitivity of our measurements to the extent of labeling of the acceptor-labeled latex, we synthesized a new latex particle sample containing 0.5 mol % NBen. We prepared 1:1 mixtures of this latex with the Phe-PBMA sample and cast films in the same way as those prepared for the experiments described in Figures 5 and 6. Experiments with this mixture showed that Φ_{ET} increased from a value of 0.09 in the newly formed film to 0.52 in the fully mixed film. As one would expect, a higher concentration of acceptor groups in the fully mixed film leads to a higher efficiency of energy transfer. Our data analysis scheme presumes that any differences in the absolute values of Φ_{ET} will be automatically accommodated when we use these data to calculate f_m values. We explore the validity of this hypothesis by comparing films containing the two different acceptor-labeled latexes.

For this comparison, we cast two set of films, the first containing a 1:1 mixture of Phe-PBMA with NBen-(0.3%)-PBMA latex and the other with a 1:1 mixture containing the NBen(0.5%)-PBMA latex. Because the rate of polymer diffusion is so sensitive to temperature, a few degrees difference in oven temperature can have a significant effect on the rate of growth of f_m. To minimize the problem of temperature reproducibility in setting the oven temperature, both sets of films were annealed simultaneously at 70 °C. The data are presented in Figure 7. One sees excellent agreement in the data, with small differences appearing only at long annealing times. We conclude that effective experiments are possible with the smaller extent of the NBen acceptor label present.

Quantifying the Rate of Polymer Diffusion. It is not possible with f_m values alone to quantify the magnitude of external variables such as temperature or the addition of plasticizer solvents on polymer diffusion rates in latex films. One needs to be able to calculate from the data a parameter that is a measure of the polymer diffusion rate. The ideal parameter would be the center-of-mass diffusion coefficient D_{cm}. For a system as complex as a latex film, in which the polymers have a broad distribution of molecular weights, calculating the distribution of D_{cm} values that characterize the system is a daunting task. In the past we have taken several approaches to this problem, including attempts to simulate the experiment[16,19−21] in terms of a single mean diffusion coefficient characterizing the distribution of polymers diffusing across the interface. Here we describe parallel approaches to the problem. First, we describe the simplest approach we have used in the past,[1,7] which involves making severe assumptions about the FRET experiment to calculate mean apparent

diffusion coefficients D_{app} as a function of the extent of diffusion in the system. In addition, we describe a new approach to simulating polymer diffusion in which we take into account the concentration profile of the polymer arising from diffusion across the particle boundary and its influence on the energy transfer signal. Both approaches calculate a single mean diffusion coefficient to describe the diffusion of a polymer characterized by a distribution of diffusivities. Since M_w for the polymer is approximately three times the entanglement molar mass M_e, and $M_w/M_n \approx 2.5$, entanglements make a relatively minor contribution to the diffusion we monitor.[22]

To begin, we need a model that describes the concentration profile of the polymer in a particle as a function of the extent of mixing between the polymer chains from neighboring particles. A useful starting point is to assume that the general shape of the polymer segment distribution can be described by Fickian diffusion profile for spherical geometry.[23] The basic model is similar to that developed in ref 16. We describe the distributions of the donor and acceptor dyes (g_D and g_A) in neighboring PBMA particles as

$$g_D(rr) = \frac{1}{2}\left(\mathrm{erf}\left(\frac{1+rr}{\theta}\right) + \mathrm{erf}\left(\frac{1-rr}{\theta}\right) + \right.$$
$$\left. \frac{\theta}{\sqrt{\pi}rr}\left\{\exp\left[-\left(\frac{1+rr}{\theta}\right)^2\right] - \exp\left[-\left(\frac{1-rr}{\theta}\right)^2\right]\right\}\right) \quad (9a)$$

$$g_A(rr) = g_D(2 - rr) \quad (9b)$$

where $\theta = 2(Dt_{dif})^{1/2}/R_s$, t_{dif} is the diffusion time, D is the diffusion coefficient, R_s is the radius of the particle, and $rr = r/R_s$ measures the distance from the center of the particle. From the distribution profiles we can calculate the volume fraction of polymer mixing f_s as

$$f_s = 1 - 3\int_0^1 4\pi r^2 g_D(rr)\,drr \quad (10)$$

The Apparent Diffusion Coefficients D_{app}. In this model, we evaluate polymer diffusion in latex films at the level of the evolution of the energy transfer quantum efficiency calculated from the experimental decay profiles with eq 6. To evaluate the mean apparent diffusion coefficient D_{app}, we begin by equating f_m (eq 8) with the fractional mass that has diffused across the interface (eq 10). While both f_m and f_s increase from 0 to 1 as the experiment proceeds, they measure different consequences of polymer diffusion. The only justification for setting $f_m = f_s$ is convenience in data analysis. We use simulations of the experiment to understand the consequences of this assumption. Previous simulations of Fickian diffusion based on a planar diffusion geometry have indicated that values of D_{app} calculated in this way are proportional to D_{cm} for values of f_m up to about 0.7.[21,24] D_{app} values calculated in this way for the data in Figure 5 are plotted against f_m in Figure 8. These values increase markedly with increasing temperature. There is also a tendency for these values to decrease with increasing f_m, which we attribute to the molecular weight polydispersity of our latex samples.

In Figure 9 the D_{app} values obtained at different temperatures are plotted in an Arrhenius fashion. In making these plots, we compare D_{app} values at similar extents of mixing. For three different values of f_m, these data can be fitted with an apparent activation energy
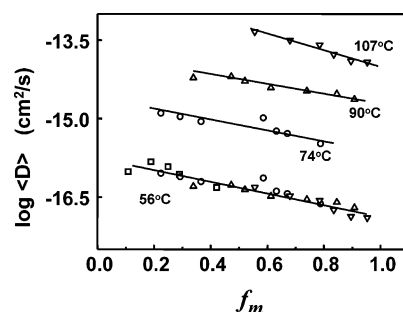
Figure 8. Apparent diffusion coefficient D_{app} vs the extent of mixing f_m at four temperatures (56, 74, 90 and 107 °C). The lowermost cure is a master curve of D_{app} values at 56 °C constructed from all of the data using the value of $E_a = 33.5 \pm 2.5$ kcal/mol. The points (□) are obtained from experimental data at 56 °C.
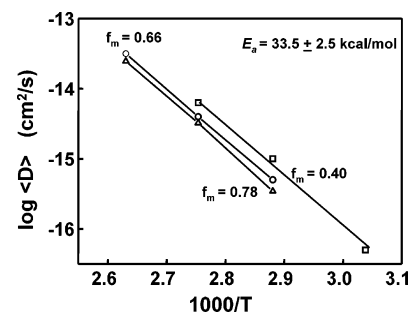

Figure 9. Arrhenius plot of log D_{app} vs $1/T$ (f_m value from top to bottom are 0.40, 0.66, and 0.78). The data compared are from similar values of f_m.

$E_a = 33.5 \pm 2.5$ kcal/mol. To emphasize the fact this value pertains to all of our data, we use this value to calculate a shift factor to create a master curve of D_{app} values at 56 °C. The shifted values calculated in this way are shown in Figure 8.

These results indicate that polymer diffusion monitored by FRET experiments with Phe/NBen as the donor/acceptor pair give very similar results to those obtained earlier with Phe/anthracene as the donor/acceptor pair. For example, the magnitudes of the D_{app} values are similar to those we have reported previously. In making this comparison, one has to keep in mind that the polymer diffusion rate is very sensitive to temperature and chain length. Thus the specific values of D_{app} calculated in any one set of experiments depend on the annealing temperature, the polymer molecular weight, and its molecular weight distribution. A more meaningful comparison is the temperature sensitivity of the diffusion rate as reflected in E_a. We previously reported values of 34 kcal/mol[1a] for a sample of PBMA of $M_w = 38\,000$ and 39 kcal/mol[2] for a PBMA sample of $M_w = 600\,000$. This difference arises as a natural consequence of the dependence of E_a on difference between the temperatures of the measurements compared to the glass transition temperature of the polymer. The two samples of different molecular weight referred to above differ in their glass transition temperatures by $10-12$ °C. Within the uncertainty of working with different sets of samples 10 years apart, we conclude that the change of dye has no influence on the polymer properties we probe.

Mean Diffusion Coefficients through Simulations. We next consider a more detailed model that describes the shape of the donor fluorescence decay profile for energy transfer between dyes attached to
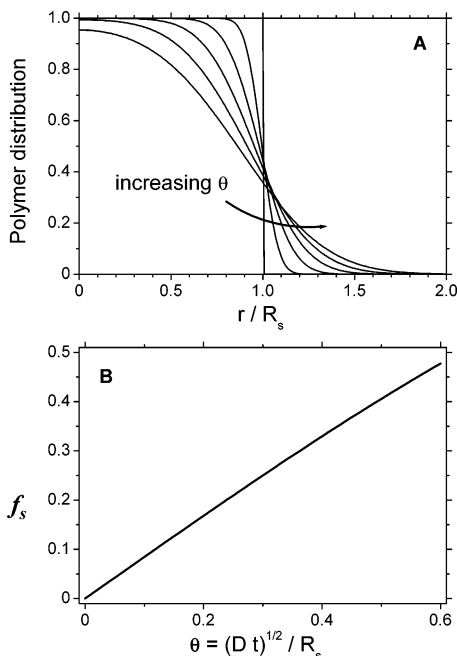
Figure 10. Polymer density distribution functions (A) in a latex particle of radius R_s, calculated using eq 9 for $\theta = 2$ ($D t_{\text{diff}})^{0.5}/R_s$ values of 0, 0.1, 0.2, 0.3, 0.4, and 0.5, as a function of distance r from the particle center. The volume (mass) fraction of mixture f_s (B) increases almost linearly with θ in the range showed.

polymer chains in latex particles forming a solid film. This type of model has been developed from first principles both for planar[21] and for spherical geometry.[15] The dyes are assumed to be attached at random to the polymer chains, so that the spatial distribution of dyes follows the segment distribution of the individual polymer chains. As the polymer chains inside the particles interdiffuse across the interface between particles, donor and acceptor dyes come into close proximity and the energy transfer between them increases. This increase can be used to determine the diffusion profile of polymer chains using a theoretical model that accounts for the diffusion of the polymer and the energy transfer from the donor to the acceptor dyes. The model has two parts. First, we use eq 9 to describe the distribution of polymer segments. This model assumes that there are no significant reptation effects in the system. In addition, one needs a kinetic model to describe the rate of direct nonradiative energy transfer for the dyes distributed according to the polymer diffusion profile. Here we introduce the concentration profiles calculated from eq 9 into eq 5 to calculate the time profiles of the survival probability of the excited donor.

The shapes of the distributions are presented in Figure 10A for increasing values of θ. From the distribution profiles we can calculate the volume (mass) fraction of polymer mixing f_s using eq 10. This parameter increases almost linearly with θ within the range of values shown (Figure 10B), providing a reliable way of calculating the diffusion coefficient from the volume fraction of mixing. For $\theta = 0.5$ the volume of polymer that diffuses past the center of the first-neighbor particles ($r/R_s = 2$) is less than 0.2% of the polymer initially in the particle. Above this θ value, the mixing of polymer chains coming from particles whose centers are at a distance $4R_s$ (second-neighbor particles) starts to become significant and would introduce a further complication into the model. Therefore, we restrict our
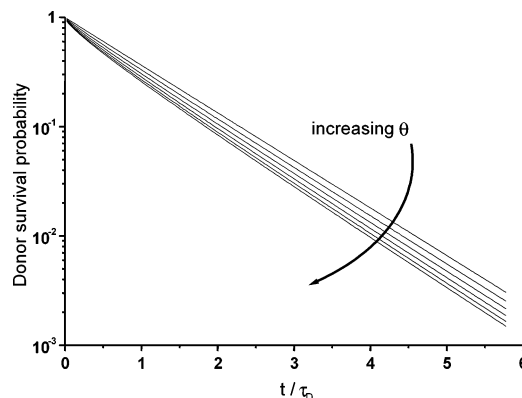
Figure 11. Simulated donor survival probability curves for $\theta = 0$, 0.1, 0.2, 0.3, 0.4, and 0.5, calculated using eqs 5 and 9. In these simulations we used $\kappa^2 = 0.476$, $R_0 = 2.37$ nm, $\tau_D = 46.1$ ns, and a minimum acceptor–donor distance $R_e = 0.5$ nm. The initial average concentration of acceptor, $C_{A0} = 0.023$ M, corresponds to the 0.3 mol % of acceptor, with 97% BMA conversion and $d_{\text{PBMA}} = 1.05$ g/cm^3.

calculations to values lower than $\theta = 0.5$, corresponding to a maximum volume fraction of mixing $f_s = 0.4$.

To relate the polymer segment density distribution across the particle boundary to the donor survival probability, we use the theory of energy transfer in restricted geometry as described in ref 16. In eq 5, $C_D(r)$ and $C_A(r)$ are the respective concentration profiles of donors and acceptors, described by eq 9. We set $C_D(r) = g_D(r)$ and $C_A(r) = C^0_A g_A(r)$, with $g_A(r)$ described by eq 9b. C^0_A is the initial average number density of acceptors in the acceptor-labeled particles. In the numerical evaluation of eq 4 using the distribution functions in eq 9, we calculate all the integrals using a simple trapezoidal rule because more sophisticated adaptive quadrature routines are not stable when used in the evaluation of multiple integrals.[25] Also, since $w(r)$ is a very sharply peaked function of r for all accessible experimental times, the integration over r in eq 5b was evaluated only from R_e to $3 R_0$.

We start by simulating a series of donor fluorescence decay functions calculated according to eqs 5 and 9, for $\theta = 0$–0.5, using $\kappa^2 = 0.476$, $R_0 = 2.37$ nm, $\tau_D = 46.1$ ns, and a cutoff distance $R_e = 0.5$ nm. The donor-labeled particle has a radius $R_s = 65$ nm, and the average concentration of the acceptor in the matrix is $C^0_A = 0.023$ M. In Figure 11 we show simulated donor survival probability curves for $\theta = 0$, 0.1, 0.2, 0.3, 0.4, and 0.5, calculated using eqs 5 and 9. These curves represent "noise-free" data obtained directly from the simulations and correspond to the donor distribution profiles shown in Figure 10. In Figure 11 we see that as the amount of mixing increases, more donors and acceptors come into proximity, and the donor decays faster, particularly at early times. We note that for $\theta = 0$ nm the donor fluorescence survival probability represents the amount of energy transfer taking place across a perfectly sharp interface.

To evaluate the extent of mixing at the interface in real samples, we compare the experimental fluorescence decay profiles obtained for the PBMA latex films at different annealing times to the simulated decays.[16] The noise-free donor decay profiles $I^s_D(t)$ calculated using eqs 5 and 9 were convoluted with the experimental instrument response functions $L(t)$, obtained from the experimental excitation source.[26] The experimental decay profiles were then fitted to each of the convoluted
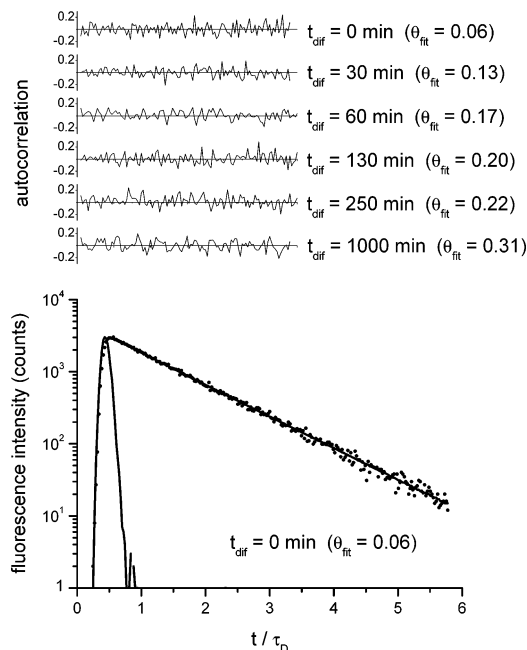
Figure 12. Experimental instrument response function and experimental donor decay profile measured for a film of PBMA (bottom), dried at room temperature and fitted to a decay simulated with $\theta = 0.06$. Autocorrelation function plots (top) for the fitting of the experimental curves of the dried film ($t_{\text{dif}} = 0$) and films annealed for 30, 60, 130, 250, and 1000 min at 56 °C, to curves simulated with $\theta = 0.06$, 0.13, 0.17, 0.20, 0.22, and 0.31.

curves, using a linear fitting algorithm where the fitting parameters are the normalization factor of the decay intensity a_N and the light scattering correction a_L.[27] To evaluate the quality of the fitting results, we calculated the reduced χ^2, the weighted residuals, and the autocorrelation of residuals.

In Figure 12 we show the experimental donor decay profile measured for a film of PBMA (bottom), freshly dried at room temperature and fitted to a decay simulated with $\theta = 0.06$. Autocorrelation function plots (top) for the fitting of the experimental curves of a film just dried ($t_{\text{dif}} = 0$) and subsequently annealed for 30, 60, 130, 250, and 1000 min at 56 °C, to curves simulated with $\theta = 0.06$, 0.13, 0.17, 0.20, 0.22, and 0.31, respectively. We fit the experimental donor decay profile starting from the beginning of the excitation profile (about 5 ns before the maximum value of the lamp profile) and obtain well-distributed autocorrelation plots of the weighted residuals for the optimal parameter values.

For all the experimental decays analyzed, the decay-intensity-normalization a_N and the light-scattering-correction a_L parameters obtained from the best fitting of the experimental data do not change significantly. Plots of the reduced χ^2 versus θ (Figure 13) for fitting of the experimental curves of the dried film ($t_{\text{dif}} = 0$) and films annealed for 30, 60, 130, 250, and 1000 min at 56 °C to curves simulated with $\theta = 0.06$, 0.13, 0.17, 0.20, 0.22, and 0.31 allow us to evaluate the sensitivity of our fitting procedure. Using this process we obtain the optimum values of θ for films annealed at different temperatures.

In Figure 14A we show the volume fraction of mixing f_s calculated by using eq 10 from the best-fit θ values obtained for films annealed at 56, 74, and 90 °C for several annealing times. For higher annealing temper-
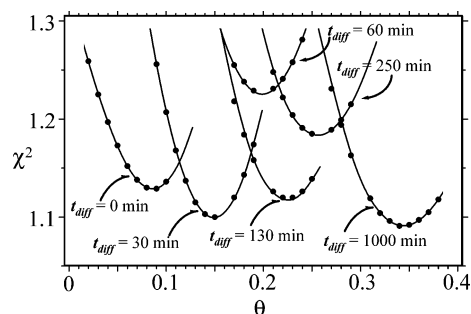
Figure 13. Reduced χ^2 plots from the fit of experimental fluorescence decay profiles obtained for the dried film ($t_{\text{dif}} = 0$) and films annealed for 30, 60, 130, 250, and 1000 min at 56 °C. The best fits are obtained for $\theta = 0.06$, 0.13, 0.17, 0.20, 0.22, and 0.31.
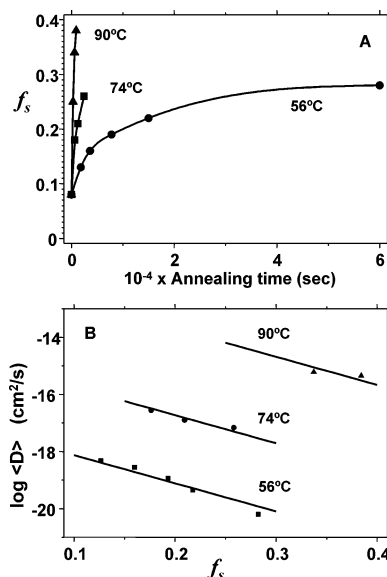
Figure 14. Volume fraction of mixing obtained for films annealed at 56, 74, and 90 °C (A) and diffusion coefficients corresponding to the fitted θ values (B). Multilinear fit of the data points corresponding to the three annealing temperatures (bottom) yields a diffusion activation energy of 38 ± 5 kcal mol^{-1}.

atures the diffusion is faster, reaching higher volume fractions of mixing within the analyzed annealing times. For the films dried a room temperature, we calculate that there is already 8% of mixing between donor- and acceptor-labeled chains before any annealing. This value can be either due to mixing of low molecular weight chains or labeled oligomers during film drying or to roughness/irregularity of the particle surface after deformation to form the transparent film.

From the best-fit θ value, it is possible to calculate an average diffusion coefficient $\langle D \rangle = (\theta R_s/2)^2/t_{\text{dif}}$ for each annealing time t_{dif}, where R_s is the initial radius of the latex particle. In Figure 14B we plot the logarithm of $\langle D \rangle$ as a function of the volume fraction of mixing f_s for films annealed at 56, 74, and 90 °C for several annealing times. The first important observation is that these $\langle D \rangle$ values decrease with increasing extent of mixing as measured by f_s. Thus using experimental fluorescence decay curves to optimize values of θ captures an essential feature of the polymer diffusion: the diffusion coefficient decreases reflecting the contribution of higher molar mass polymers to the growth in FRET at later times in the experiment. In addition, we note that $\langle D \rangle$ values increase with increasing temperature. We fit the

data in Figure 14B to three parallel lines to obtain $\langle D \rangle$ values at comparable extents of mixing.[28] When these values are analyzed in an Arrhenius fashion, we obtain an effective activation energy for diffusion of 38 ± 5 kcal mol^{-1}.

Comparing the Two Data Analysis Methods. In this section, we compare quantitatively the two different methods of data analysis, the simple approach (the "f_m method"), based on calculation of f_m from experimental values of Φ_{ET}, and the more rigorous approach (the "f_s method") in which one uses simulations based on eqs 5 and 9 to parametrize individual donor decay profiles. As we will see, these two methods yield diffusion coefficients with values that can differ significantly. We show, however, that for virtually all experiments of interest, this difference is not an order of magnitude but closer to a factor of 2–4. We carry out this comparison in two ways.

Simulations in which *D* Is Constant. We begin by calculating and comparing f_m and f_s values, using simulated data based on a single-valued diffusion coefficient D as our point of reference. The overall strategy is relatively simple. First, we choose values of the diffusion parameter θ characteristic of our experiments. For a given value of $\theta = 2(Dt_{dif})^{1/2}/R_s$, we calculate the corresponding donor and acceptor concentration profiles (eq 9). From these curves, we calculate values of the volume (mass) fraction of mixing f_s with eq 10. These concentration profiles also serve as input data to eq 5 to evaluate the simulated excited-donor survival probability curves $I_D^s(t)$. The energy transfer efficiencies Φ_{ET} are calculated by inserting $I_D^s(t)$ into the numerator of eq 6 and carrying out the integration.

We first consider an initially sharp interface between neighboring particles and simulate the polymer interdiffusion between the particles as described in the preceding paragraph. To calculate values of f_m, we normalize the energy transfer efficiency using its value for a sharp interface $\Phi_{ET}(t_0)$ and for a completely mixed film $\Phi_{ET}(t_\infty)$.[27] We assume the completely mixed film to be homogeneous, calculate the corresponding $I_D^s(t)$ with eqs 3 and 4, and evaluate $\Phi_{ET}(t_\infty)$ from eq 6. Under these conditions both f_m and f_s are equal to zero at $t_{dif} = 0$, so their ratio is indeterminate. The first increment of diffusion makes a significant contribution to the increase in Φ_{ET}. Thus f_m is initially much larger than f_s, as one can see for small values of θ in Figure 15A, and remains larger than f_s over the entire "experiment". The ratio f_m/f_s decreases rapidly for values of θ up to 0.05 (inset in Figure 15A), with a mild subsequent decrease to reach a value of 1.5 at $\theta = 0.5$. As expected for Fickian diffusion, f_s increases linearly with $t_{dif}^{1/2}$. In contrast, f_m exhibits a small downward curvature. Previous simulations employing a planar geometry and a constant diffusion coefficient showed f_m increasing approximately linearly with $t_{dif}^{1/2}$ up to $f_m \approx 0.7$.[21] Thus there is more curvature in the f_m vs $t_{dif}^{1/2}$ plot for simulations in spherical geometry than in planar geometry.

The results in Figure 15A suggest that we plot experimental values of f_m against $\theta = 2 (D_{app}t_{dif})^{1/2}/R_s$. We show the plot in Figure 16 for data obtained at several annealing temperatures. On the scale of $f_m = 0$–1, the plot appears to be linear up to $f_m \approx 0.7$. However, upon closer inspection (Figure 16 insert), one can see a slight downward curvature at lower f_m values.
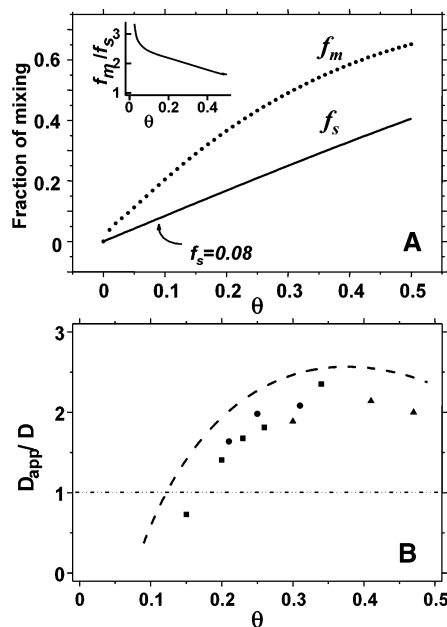
Figure 15. (A) Comparison of f_m and f_s values as a function of θ obtained from a simulation involving a single-valued diffusion coefficient and an initially sharp interface between the donor- and acceptor-labeled domains. The inset shows a plot of the ratio f_m/f_s against θ. The arrow at $f_s = 0.08$ refers to the amount of mixing found experimentally in latex films freshly prepared at room temperature. (B) The dashed line refers to values of the ratio D_{app}/D_n plotted against θ, in which both values were obtained from a simulation similar to that described in A, except that the initial conditions for the calculation of both D values were modified to take into account the amount of diffusion ($f_s(t_0) = 0.08$) that appears to take place during film drying. The discrete points refer to ratios of experimental D_{app} values (see Figure 8) to values of $\langle D \rangle_n$ obtained through fitting the experimental donor decay curves to the simulated curves. The approach was similar to that used to obtain the data in Figure 13, except that the initial conditions for the calculations were modified to take account of $f_s(t_0) = 0.08$. The individual data points refer to experiments carried out at annealing temperatures of 56 (■), 74 (●), and 90 °C (▲) for various annealing times.
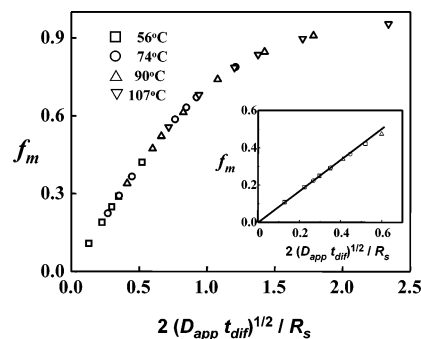
Figure 16. Plot of the data in Figure 8 in the form of f_m against $\theta = 2(D_{app}t_{dif})^{1/2}/R_s$.

In a real experiment, there is an oligomer component that diffuses rapidly and increases the value of $\Phi_{ET}(t_0)$ to a value greater than that predicted for a sharp interface. In the preceding section, we concluded that approximately 8% of mixing between donor- and acceptor-labeled polymer took place as the films dried, so that at $t_{diff} = 0$ we have $f_s(0) = 0.08$. The oligomer raises the background energy transfer signal but makes no further contribution to the experimental data. In analyzing experimental data, we take account of this signal in the calculation (eq 8) of f_m by subtracting it from experi-

mental values of $\Phi_{ET}(t_{dif})$ and $\Phi_{ET}(t_\infty)$. The challenge is to incorporate this contribution to the FRET signal into our simulations.

To compare D and D_{app}, we will treat the value f_s (0) = 0.08 as the initial state for diffusion and use eqs 9 and 10 to recalculate the best value of the normalized diffusion coefficient D_n that describes the subsequent increase in f_s. The new normalized volume fraction of mixing $f_s{}^n(t_{diff}) = [f_s(t_{diff}) - f_s(0)]/[1 - f_s(0)]$ approximately corresponds to the amount of diffusion we would have if the magnitude of $\Phi_{ET}(t_0)$ following drying of the films were treated as due to surface roughness of the particles and the concentration profile corresponding to $f_s(0)$ was the boundary condition to solve the Fickian diffusion equation.

For this comparison, we calculate D_{app} by setting f_m from the simulation equal to f_s and proceeding as described above for the experimental values of f_s. In Figure 15B, we compare the two types of diffusion coefficients. The dashed line refers to the ratios of these calculated values of D_{app} and D_n. This ratio is initially small and increases to about $D_{app}/D_n = 2.5$ at $\theta = 0.4$.

Simulations in Which D Evolves with θ. In this analysis, we compare experimental values of D_{app} to simulated values of $\langle D \rangle$. This comparison would be straightforward if we were to take as the initial state (as in Figure 13) a sharp interface between donor- and acceptor-labeled domains. As in the previous section, we attempt to accommodate the background energy transfer due to oligomer diffusion, recalculate average normalized diffusion coefficients $\langle D \rangle_n$ values based on renormalized volume fraction of mixing values $f_s{}^n(t_{diff}) = [f_s(t_{diff}) - f_s(0)]/[1 - f_s(0)]$ using the initial value $f_s(0) = 0.08$. In Figure 15B we show a series of points corresponding to the ratio of experimental D_{app} values to the simulated $\langle D \rangle_n$ values that best fit the experimental donor decay curves. The different symbols refer to experimental data obtained at 56, 74, and 90 °C. These points follow the dashed line remarkably well. We conclude that for the parameters associated with our experiment, values of D_{app} reasonably approximate the polymer diffusion coefficients within a factor of 2−4. We plan to look into the dependence of $D_{app}/\langle D \rangle_n$ on the initial mixing state and other variables in a future publication.

We see that the simple f_m method, in which one calculates D_{app} values from f_m, yields different values of the diffusion coefficient than the physically more appropriate f_s method. In the second model, one solves a diffusion equation to generate concentration profiles and uses these to carry out mathematical simulations of the energy transfer experiment. Within the assumptions of the model (spherical geometry, Fickian diffusion) one can calculate via eq 10 the actual mass or volume fraction of polymer (f_s) that has diffused across the interface over time. The f_m method is simpler. Even though it yields apparent diffusion coefficients that differ in value from the true diffusion coefficients, it can still account for the temperature dependence of the polymer diffusion rate.

Summary

We described experiments in which direct nonradiative energy transfer measurements were used to monitor polymer diffusion in PBMA latex films with a polymer molar mass of $M_w \approx 125\,000$ ($M_w/M_n = 2.5$). These experiments employed the nonfluorescent accep-tor chromophore NBen, which allowed faster data acquisition at lower acceptor dye concentration (0.3, 0.5 mol %) than previous experiments with anthracene (1 mol %) as the acceptor. The data were analyzed in two distinct ways. Our traditional simplified approach involved calculating f_m values from the quantum efficiencies of FRET (Φ_{ET}). Apparent diffusion coefficients D_{app} were calculated by the "f_m method" that makes rather severe assumptions about f_m and the amount of polymer that has diffused across the interparticle interface. These D_{app} values and their temperature dependence were similar to those obtained a decade ago using anthracene as the acceptor.

In addition, we carried out mathematical simulations of diffusion that satisfied Fick's laws in a spherical geometry. The concentration profiles of donor and acceptor were introduced into equations that describe the rate of energy transfer, and donor decay profiles were simulated. By comparing simulated and experimental decay profiles as a function of sample annealing time, "the f_s method", optimum values of the mean diffusion coefficient $\langle D \rangle$ were obtained.

A comparison of the two different methods of data analysis indicates that D_{app} values are larger than $\langle D \rangle$ values by a factor of 2−4 but track the "true" diffusion coefficients rather well. From the temperature dependence of the diffusion coefficients, we found effective activation energies for diffusion of $E_a = 33.5 \pm 2.5$ kcal/mol from D_{app} and 38 ± 5 kcal/mol from $\langle D \rangle$. The E_a values determined here are in reasonable agreement with the energy ($E_a = 39$ kcal/mol) that we obtained in experiments that used anthracene as the acceptor dye and with the value of the apparent activation ($E_a = 37$ kcal/mol) obtained by the Ferry group more than 50 years ago for creep compliance measurements on PBMA in this range of temperatures.[29]

References and Notes

(1) (a) Zhao, C. L.; Wang, Y. C.; Winnik, M. A. *Macromolecules* **1990**, *23*, 4082. (b) Wang, Y. C.; Zhao, C. L., Winnik, M. A. *J. Chem. Phys.* **1991**, *95*, 2143.
(2) Wang, Y. C.; Winnik, M. A. *J. Phys. Chem.* **1993**, *97*, 2507.
(3) (a) Feng, J. R. Ph.D. Thesis, University of Toronto, Canada, 1996. (b) Odrobina, E. Ph.D. Thesis, University of Toronto, Canada, 2000.
(4) Feng, J.; Winnik, M. A. *Macromolecules* **1997**, *30*, 4324.
(5) Kawaguchi, S.; Odrobina, E.; Winnik, M. A. *Macromol Rapid Commun.* **1995**, *16*, 861.
(6) Wang, Y. C.; Winnik, M. A.; Haley, F. *J. Coat. Technol* **1992**, *64* (811), 51.
(7) (a) Kim, H. B.; Winnik, M. A. *Macromolecules* **1994**, *27*, 1007. (b) Kim, H. B.; Winnik, M. A. *Macromolecules* **1995**, *28*, 2033−2041.
(8) (a) Oh, J. K.; Wu, J.; Winnik, M. A.; Craun, G. P.; Rademacher, J.; Farwaha, R. *J. Polym. Sci. Part A. Polym. Chem.* **2002**, *40*, 1594. (b) Oh, J. K.; Wu, J.; Winnik, M. A.; Craun, G. P.; Rademacher, J.; Farwaha, R. *J. Polym. Sci. Part A. Polym. Chem.* **2002**, *40*, 3001.
(9) Zhou, C. L.; Winnik, M. A.; Jao, T. C. *J. Polym. Sci. Part A. Polym. Chem.* **2001**, *39*, 2642.
(10) Liu, Z. Q.; Winnik, M. A.; Jao, T. C.; Rösch J. *J. Phys. Chem. A* **1998**, *102*, 5349.
(11) O'Connor, D. V.; Phillips, D. *Time-Correlated Single Photon Counting*; Academic Press: London, 1984.
(12) Förster, Th. *Ann. Phys. (Leipzig)* **1948**, *2*, 55. Förster, Th. *Z. Naturforsch* **1949**, *4a*, 321.

(13) Lakowicz, J. R. *Principles of Fluorescence Spectroscopy*, 2nd ed.; New York, 1999.

(14) Baumann, J.; Fayer, M. D. *J. Chem. Phys.* **1986**, *85*, 4087.

(15) Blumen, A.; Klafter, J.; Zumhofen, G. *J. Chem. Phys.* **1986**, *84*, 1397. Treat the case in which all donors are related by symmetry.

(16) Farinha, J. P. S.; Martinho, J. M. G.; Kawaguchi, S.; Yekta, A.; Winnik, M. A. *J. Phys. Chem.* **1996**, *100*, 12552.

(17) Martinho, J. M. G.; Farinha, J. P. S.; Berberan-Santos, M. N.; Duhamel, J.; Winnik, M. A. *J. Chem. Phys.* **1992**, *96*, 8143.

(18) de Gennes, P. G. *Scaling Concepts in Polymer Physics*; Cornell University: Ithaca, NY, 1979.

(19) Winnik, M. A.; Li, L.; Liu, Y. S. In *Microchemistry: Spectroscopy and Chemistry in Small Domains*; Masuhara, H., Kitamura, N., Eds.; Elsevier: Holland, 1994; p 389.

(20) Winnik, M. A.; Liu, Y. S. *Makromol. Chem. Makromol. Symp.* **1995**, *92*, 321.

(21) Farinha, J. P. S.; Martinho, J. M. G.; Yekta, A.; Winnik, M. A. *Macromolecules* **1995**, *28*, 6084.

(22) Odrobina, E.; Winnik, M. A. *Macromolecules* **2001**, *34*, 6029.

(23) Crank, J. *The Mathematics of Diffusion*; Clarendon: Oxford, 1975.

(24) Dhinojwala, A.; Torkelson, J. M. *Macromolecules* **1994**, *27*, 4817.

(25) Lyness, J. N. *SIAM Rev.* **1983**, *25*, 63.

(26) Farinha, J. P. S.; Martinho, J. M. G.; Pogliani, L. *J. Math. Chem.* **1997**, *21*, 131.

(27) Farinha, J. P. S.; Vorobyova, O.; Winnik, M. A. *Macromolecules* **2000**, *33*, 5863.

(28) In this linear regression analysis we fit straight lines with the same slope but different values at the origin.

(29) Child, W. E.; Ferry, J. D. *J. Colloid Sci.* **1957**, *12*, 327.